B_c-meson production in ultrarelativistic nuclear collisions

Martin Schroedter, Robert L. Thews, and Johann Rafelski
Department of Physics, University of Arizona, Tucson, Arizona 85721
(Received 7 April 2000; published 20 July 2000)

We study quantitatively the formation and evolution of $\overline{bc}$, $b\overline{c}$ bound states in a space-time domain of deconfined quarks and gluons (quark-gluon plasma, QGP). At the Relativistic Heavy Ion Collider (RHIC), one expects for the first time that typical central collisions will result in multiple pairs of heavy (in this case charmed) quarks. This provides a new mechanism for the formation of heavy quarkonia which depends on the properties of the deconfined region. We find typical enhancements of about 500-fold for the $\overline{bc}$, $b\overline{c}$ production yields over expectations from the elementary coherent hadronic B_c-meson production scenario. The final population of bound states may serve as a probe of the plasma phase parameters.

PACS number(s): 12.38.Mh, 14.40.Nd, 25.75.−q

I. INTRODUCTION

The recent observation of candidate B_c-meson events by the CDF Collaboration [1] yields measurements for the ground state mass and lifetime which are consistent with expectations from nonrelativistic potential models [2]. This system of states is expected to have properties intermediate between the J/ψ and Υ systems (except for its longer lifetime due to the absence of quark annihilation processes). Thus it is natural to investigate the fate of such states when produced in a deconfined environment, where suppression relative to ''expected'' yields may serve as a signature for the existence of deconfinement.

We have previously reported some preliminary work toward this end [3,4]. Our calculations of the expected yield of B_c at the Relativistic Heavy Ion Collider (RHIC) utilize estimates of the coherent production of both a $b\overline{b}$ and $c\overline{c}$ pair in the same initial hard perturbative quantum chromodynamics (QCD) process, followed by hadronization into the B_c states. This process is of order α_s^4, and falls quite rapidly with decreasing energy. The resulting prediction at RHIC energies for the bound-state fraction relative to initial b-quark production is in the range $10^{-4}-10^{-5}$ [5]. Combining this result with the expected yield of b quarks, we find that even at design luminosity there will be at most a handful of B_c mesons produced at RHIC which decay into observable final states (all scalar, vector, excited, particle/antiparticle $\overline{bc}$ bound states will be called B_c-mesons or simply B_c, except when otherwise noted). Thus a scenario of production via calculable hard QCD interactions followed by suppression in a deconfined medium will be irrelevant for RHIC parameters.

What we now present is a new production mechanism which itself depends on the existence of a deconfined state. The new mechanism becomes relevant for the first time at RHIC energies, since typical central collision events will have multiple pairs of initially produced charm quarks. Estimates using perturbative QCD to calculate the initial production of heavy quarks predict approximately 10 $c\overline{c}$ pairs in each central event in Au-Au collisions at $\sqrt{s}=200$ GeV [6]. Due to the larger mass, only about one in 20 central events will produce a $b\overline{b}$ pair.

Consider the events in which there is a single $b\overline{b}$ pair, along with the expected 10 $c\overline{c}$ pairs. If a region of deconfined matter is subsequently produced in the space-time region encompassing the heavy quarks, a b-quark will be able to ''find'' any of the initially produced charm quarks with which to produce the final B_c bound state. More generally, our study shows that the formation of quarkonium states within a deconfined space-time domain resulting from the interaction of mobile heavy quarks offers a very interesting signature for deconfinement.

In Sec. II we study quantitatively the probability that in the deconfined quark-gluon plasma (QGP) phase the mobile c, $\overline{c}$-quarks can seek, find, and bind to a $\overline{b}$, b quark produced in the same event. We also consider the dynamical evolution of these heavy quark bound states in the deconfined phase. In Sec. II A we establish the kinetic model for the evolution in time of the $\overline{bc}$, $b\overline{c}$ bound state population. The required cross sections are presented in Sec. II B, and the formation and dissociation reaction rates obtained [7].

To calculate the final B_c yield, one needs an estimate of the charm quark *density* during the deconfined phase. We therefore consider in Sec. III A a generic model for the expansion and cooling of the QGP. This also enables the comparison of direct (initial) and microscopic thermal charm production in Sec. III B. We confirm that at RHIC energy charm is produced primarily in the initial parton interactions, with only a minor contribution arising from the thermal plasma processes. We also show that the charm density at hadronization remains significantly in excess of that which would be present if full chemical equilibrium were reached.

We then present in Sec. IV a study of the influence of the model parameters on the pattern of B_c production at RHIC. We present in Sec. IV B the fractional yield per initial bottom quark pair in QGP. We find that the final yield is most sensitive to the initial charm density, and there is very little dependence on the initial temperature of the dense deconfined state. In contrast, we show in Sec. IV D that the relative yield of the first radially excited state to the ground state, $B_c(2S)/B_c(1S)$ is significantly more dependent on the initial temperature in the plasma phase.

II. CHEMICAL KINETICS OF QUARKONIUM ABUNDANCE

In our scenario, the $b\bar{c}$ and $\bar{b}c$ states formed in the QGP will be subject to collisions with gluons, which will dissociate them into their constituent quarks. This mechanism can be thought of as the dynamic counterpart of the plasma screening scenario, in which the color-confinement force is screened away in the hot dense plasma [8,9]. We do not distinguish between the vacuum and plasma values for the mass and binding energy of the $1S$ ground states. Both are significantly larger than typical temperatures expected at RHIC. Estimates for their behavior as a function of screening mass have been made [10], and indicate that such an approximation is reasonable. Thus we no longer distinguish between the plasma bound states and the physical B_c mesons which can be observed after hadronization.

The primary formation mechanism is just the inverse of the breakup reaction, in which unbound heavy quarks are captured in the bound states, emitting a color octet gluon. The competition between the rates of these reactions integrated over the lifetime of the QGP then determines the final B_c populations. Note that in this scenario it is impossible to separate the formation process from the breakup (suppression) process. Both processes occur simultaneously, in contrast to the situation in which the formation only occurs at the initial times before the QGP is present. (Of course, one can include this case also in our scenario by adjusting the initial conditions. However, for the case of B_c initial production at RHIC, we have already shown that this possibility is negligible.) A number of other reactions involving b quarks are possible in the QGP, but the rates are much smaller than those above. For example, formation of bound states with light quarks, B_s, B_u, B_d, are not possible at the high initial temperatures expected at RHIC since their lower binding energies prevents them from existing in a hot QGP, or equivalently they are ionized on very short time scales. They will be formed predominantly at hadronization, but this process is too late to affect the final B_c population. We also neglect the decrease in b-quark population due to $b\bar{b}$ annihilation into light quarks or formation of Υ states. Both of these processes depend quadratically on the b-quark densities, and proceed too slowly or too rarely, respectively, to be significant. We also neglect the breakup cross section due to collisions with light quarks, since their population in the QGP is expected to be very much suppressed relative to gluons as compared to chemical equilibrium values during the early times when the breakup reaction rate has its most significant effect [11].

A. Chemical rate equations

The abundance of bottom and charm quarks and their bound states is thus governed by very simple master (population) equations involving only two reactions. Specifically, the formation reaction F

$$b+\bar{c}\rightarrow B_c+g,$$

and the dissociation reaction D

$$B_c+g\rightarrow b+\bar{c},$$

and similar equations for the conjugate states determine the time evolution of the number of bound states in the deconfined region, N_{B_c}:

$$\frac{dN_{B_c}}{d\tau}=\lambda_F N_b\,\rho_{\bar{c}}-\lambda_D N_{B_c}\,\rho_g\,. \tag{1}$$

Since the total number of b quarks does not change under the assumptions above, the rate of change in the number of unbound b quarks N_b is just the negative of that for the number of bound state B_c mesons:

$$\frac{dN_b}{d\tau}=\lambda_D N_{B_c}\,\rho_g-\lambda_F N_b\,\rho_{\bar{c}}. \tag{2}$$

In Eqs. (1) and (2), τ is the proper time in a small volume cell, ρ_i denotes the number density $[L^{-3}]$ of species i, and the reactivity λ $[L^3/\text{time}]$ is the momentum distribution averaged reaction rate:

$$\lambda\equiv\langle\sigma v_{\rm rel}\rangle=\frac{\int\int d^3p_1\,d^3p_2\,f_1(p_1)f_2(p_2)\,\sigma(\sqrt{s})v_{\rm rel}}{\int\int d^3p_1\,d^3p_2\,f_1(p_1)f_2(p_2)}. \tag{3}$$

Note that even though λ and ρ are not Lorentz invariant, their product, the rate of particle production, is invariant. Thus, we evaluate the rates $\rho_i\,\lambda_{D/F}$ in the volume cell frame, where the (local) densities are given by external inputs.

We study here the deconfined period during which parton distributions have kinetically (but not necessarily chemically) equilibrated. We thus consider an isotropic medium of mobile quarks and gluons with the momentum distribution function f_i for particle i given by the thermal equilibrium distribution $f=(e^{E/T}\pm 1)^{-1}$. σ is the spin- and color-averaged total cross section for the relevant reaction which depends only on $s=(p_1+p_2)^2$, and $v_{\rm rel}$ is the relative speed between the two reacting particles. Except where otherwise indicated ρ_g is assumed to be in chemical equilibrium. $\rho_{\bar{c}}$ will be determined by its own kinetic equation described in Sec. III B. The spatial distribution of charm and bottom quarks will be taken to be uniform, an approximation which indicates the accuracy to which we will pursue our following calculations.

B. In-plasma cross section and reaction rates

We now need to estimate the cross sections involved in the formation and breakup reactions. For these purposes, we first utilize a derivation based on the interaction of a gluon field with the color dipole moment of a nonrelativistic heavy quarkonium state. It is implemented via an operator product expansion technique [7], and has been applied to the J/ψ breakup rates in a QGP [9]. We generalize this result to any

heavy quarkonium 1*S* state with arbitrary flavor content, so that the spin and color averaged dissociation cross section is written

$$\sigma_{\mathrm{D}}=\frac{2\pi}{3}\left(\frac{32}{3}\right)^2\left(\frac{2\mu}{\epsilon}\right)^{1/2}\frac{k_0^{7/2}}{4\mu^2}\,\frac{(k-k_0)^{3/2}}{k^5}. \tag{4}$$

Here k is the gluon momentum (in the quarkonium-rest frame), k_0 is the minimum value required to impart the binding energy ϵ to the bound state, and μ is the reduced mass. This form is valid if the quarkonium system has a spatial size small compared with the inverse of Λ_{QCD}, and its bound state spectrum is close to that in a nonrelativistic Coulomb potential with ϵ large compared with Λ_{QCD}. These conditions are marginally satisfied for the J/ψ, and should be somewhat better for the B_c kinematics. The form above has also been altered to account for recoil of the finite mass system, since in the original form the values of ϵ and k_0 were identical.

We use values $m_b=5.8$ GeV and $m_c=1.3$ GeV which are consistent with typical potential model fits to the spectra. The magnitude of the cross section is controlled by the geometrical factor $(4\mu^2)^{-1}$, which for these quark masses is consistent with the size of the bound state wave function in the same potential models. The rate of increase just above threshold is due to phase space and the *p*-wave color dipole interaction, and it reaches a maximum value for B_c dissociation of about 1.5 mb when $k=\frac{10}{7}\,k_0$. For our model calculations we use a central value of 6.3 GeV for the B_c mass, and a binding energy of 0.84 GeV which follows from the hadronic open flavor *B*- and *D*-meson masses. We retain these values for our kinetic calculations, as an approximation for physical values in the QGP. One might expect that both would decrease somewhat in a QGP. Some potential model calculations utilizing screening indicate the magnitude of this effect is expected to be small for the B_c at RHIC conditions [10].

Our dominant formation cross section σ_{F} can then be directly obtained from σ_{D} by utilizing the detailed balance relation. This is written in the zero-momentum (ZM) frame of two-body interactions as

$$(\sigma\,\mathbf{p}^2\,g)_{\mathrm{D}}=(\sigma\,\mathbf{p}^2\,g)_{\mathrm{F}}, \tag{5}$$

where $\mathbf{p}_{\mathrm{D/F}}$ is the three-momentum of the initial state particles for these reactions in their respective ZM frames, and $g_{\mathrm{D/F}}$ is the statistical degeneracy in the two channels. In the present case of an unpolarized QGP, $g_{\mathrm{D}}=((3+1)\cdot 1)(2\cdot 8)$, counting spin and color multiplicities of B_c color-singlet and gluon, and $g_{\mathrm{F}}=(2\cdot 3)(2\cdot 3)$, counting spin and color multiplicities of the initial state *b* and *c* quarks. In this formalism we have included both the pseudoscalar and vector 1*S* B_c states with the same cross sections, since in the nonrelativistic approximation one would expect the same spatial wave function and no spin dependence. These two states are also included in the no-deconfinement scenario initial production estimates [5], so that a direct comparison can be made. Using these formation-dissociation cross sections we calculate the reactivities as defined by Eq. (3). As shown in Fig. 1, formation and dissociation tend to balance at very high temperature, where the endotherm nature of the dissociation is negligible. At temperatures in the range 150–300 MeV the formation reactivity dominates by about a factor of 4.

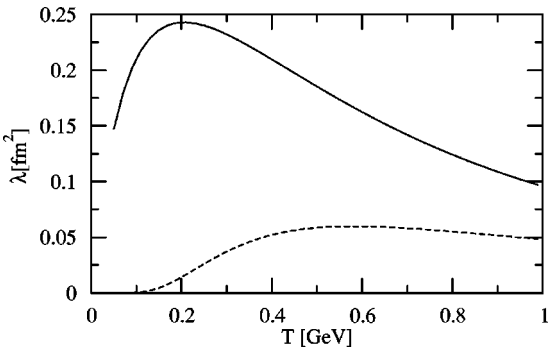

FIG. 1. Formation λ_{F} (solid) and dissociation λ_{D} (dashed) reactivities as a function of temperature.

C. B_c dissociation time scales

From Eq. (1), one sees that if the system is at a constant temperature (or equivalently the reaction rates are sufficiently fast), the final ratio of bound state to free quark populations is just given by the ratio $(\lambda_{\mathrm{F}}\rho_c^2)/(\lambda_{\mathrm{D}}\rho_g)$. The relevant time scales are set by the magnitudes of either factor in this ratio. We have calculated the dissociation rates of several quarkonium states under breakup by gluons with full chemical equilibrium density, and the results are shown in Fig. 2.

As expected, these rates rise quite sharply with temperature. The B_c curve fits quite nicely between those for the J/ψ and Υ, also as expected. We also show the same calculation for the B_s state, although the approximations made for this cross section have a very marginal validity in view of such a large state with small binding energy. For the B_c, one sees that in the range of initial temperatures expected at RHIC (roughly 300 to 500 MeV), these dissociation rates imply time scales of order 1–10 fm/*c*. Since the total QGP lifetimes

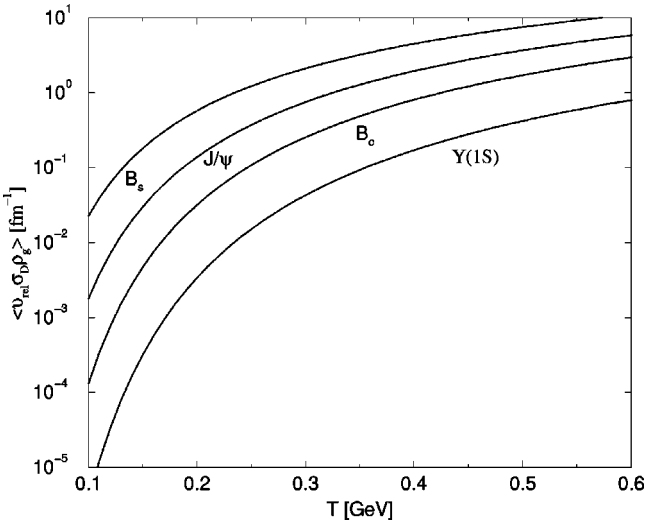

FIG. 2. Thermal QGP quarkonium dissociation rates by thermal gluons as functions of temperature.

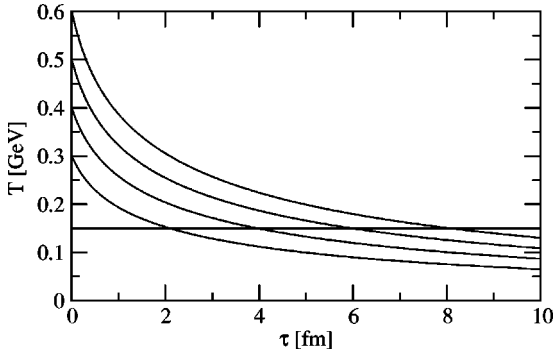

FIG. 3. Temperature [GeV] vs proper time [fm] for various initial temperatures T_0, with parameters: $l_i=1$ fm, $v_r=0.58$. The horizontal line marks hadronization.

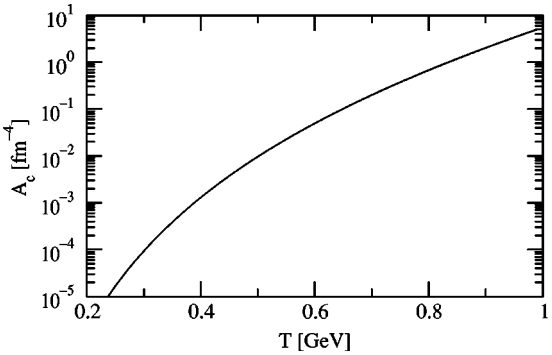

FIG. 4. (Invariant) charm production rate per unit of time and volume $A_c[T]$ as a function of temperature T.

are also in this region, it is evident that the equilibrium solutions will not in general be reached at each temperature, and one must solve the rate equations numerically to obtain the final populations.

III. EVOLUTION OF CHARM DENSITY IN QGP

A. Evolution of temperature

In order to obtain the chemical evolution of quark bound state abundances in QGP we need to establish a relation between plasma temperature and proper time. We assume that the expansion of the QGP follows an isentropic path [12]. We utilize a generic scenario for the proper-time dependence of the volume involving both longitudinal and transverse expansion, and examine the sensitivity of our final results to variations in the parameters involved. As a specific example we consider an adiabatically expanding homogeneous QGP domain having the shape of an ellipsoid of revolution about the longitudinal axis with semimajor and semiminor axes parametrized with an initial length $l_i/2=\tau_0$ and an initial transverse radius r_i. These are fixed at the time of QGP equilibration at an initial temperature T_0, when our formation and breakup reactions are assumed to start. We will explore the range $0.5<l_i<2$ fm (equivalent to thermalization times between 0.25 and 1.0 fm), and take $r_i=5$ fm for Au–Au collisions at RHIC, corresponding to 15–20 % most central interactions. The longitudinal growth occupies the region between the (almost unstopped) receding nuclei. For transverse growth we allow a radial expansion at a speed v_r. The speed of sound in an ideal relativistic gas $v_r\simeq 0.58\ c$ is taken as a nominal value, but the effects of significant variations in parameter space will be considered. Thus the volume evolves as a function of proper time τ according to

$$V(\tau)=\frac{4\pi}{3}(r_i+v_r\,\tau)^2\left(\frac{l_i}{2}+\tau\right). \tag{6}$$

Note that we have rescaled the initial proper time to zero.

This simple approach produces temperature vs time profiles which appear to be very similar to those arising in more complex studies. These are shown in Fig. 3 for a homogeneous bulk QGP state in a range of initial temperatures $0.3\leqslant T_0\leqslant 0.6$ GeV. Intersection with the horizontal line at freeze-out temperature $T_f=0.15$ GeV indicates the QGP lifespan between thermalization and hadronization.

B. Thermal charm production in QGP

From fits to experimental nucleon–nucleon reaction data it is estimated that at RHIC there will be an average number $N_{c_0}=10$ of directly produced $c\bar{c}$ pairs per central collision [6], and this is the standard value for which our calculations will be carried out. However, additional charmed quarks could be produced in the QGP by collisions of gluons:

$$g+g\rightarrow c+\bar{c},$$

and of light quarks:

$$q+\bar{q}\rightarrow c+\bar{c}.$$

The local evolution of charm density ρ_c can be described in a fashion quite similar to the model developed for strangeness production, see, e.g., [13]. Allowing for charm production and volume dilution under adiabatic expansion, the local charm density obeys

$$\frac{d\,\rho_c}{d\,T}=\frac{A_c[T]}{\dot{T}}\left(1-\left(\frac{\rho_c[T]}{\rho_c^{\infty}[T]}\right)^2\right)+3\,\rho_c\frac{1}{T}, \tag{7}$$

where $\dot{T}\equiv dT/d\tau$. The rate of charm production is

$$A_c[T]=\tfrac{1}{2}\rho_g^{\infty 2}\lambda^{gg\rightarrow c\bar{c}}+\rho_q^{\infty 2}\lambda^{q\bar{q}\rightarrow c\bar{c}}, \tag{8}$$

where ρ^{∞} denotes the density in thermal and chemical equilibrium. $A_c[T]$ is shown in Fig. 4, obtained with running QCD parameters, $\alpha_s(M_Z)=0.118$, $m_c(1\ \text{GeV})=1.5$ GeV [14].

Integrating Eq. (7), we obtain the total number of charmed quark pairs in plasma at freeze-out, with initial temperature T_0 being a parameter, along with the initial longitudinal size l_i. Figure 5 shows our results for three different initial longitudinal sizes $l_i=2$ fm (dotted), $l_i=1$ fm (dashed), and $l_i=0.5$ fm (solid): the three thick up-curving lines include both the ten directly produced charm pairs and the QGP charm production. The larger the initial volume and

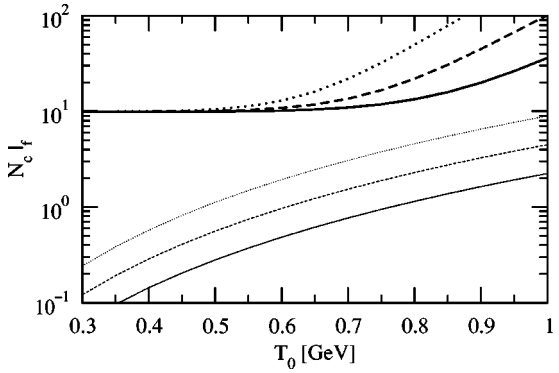

FIG. 5. Thick lines: N_c at freeze-out as a function of initial temperature T_0 [GeV]: thermally produced charm is combined with $N_{c0}=10$ charm pairs from direct initial production. Longitudinal sizes are $l_i=2$ fm (dotted), 1 fm (dashed), and 0.5 fm (solid); other parameters are the same as Fig. 3. Thin lines: chemical equilibrium abundance at freeze-out, $V\rho_c^{\infty}|_{T_f}$.

the longer the lifespan at high temperature, the greater is the QGP contribution to charm yield.

For the range of initial temperatures expected at RHIC, ones sees that there is virtually no additional charm produced in the QGP, and also that charm annihilation processes are too slow to significantly reduce the initially produced number of charm quark pairs. The thin lines show for comparison the number of charm quarks which would follow from a chemical equilibrium density at the hadron freeze-out temperature $T_f=0.15$ GeV for $m_c=1.5$ GeV. (This value depends on the initial temperature T_0 through its effect on the freeze-out volume.) The chemical equilibrium value is always significantly smaller than the corresponding direct + thermally produced abundance, i.e., direct initial charm production at RHIC is predicted in general to significantly oversaturate the statistical phase space at freeze-out.

IV. DISCUSSION OF RESULTS

A. B_c survival in plasma

To see what temperature range contributes to breakup, Fig. 6 shows the survival probability of one B_c meson being placed in the QGP at different initial temperatures. At low

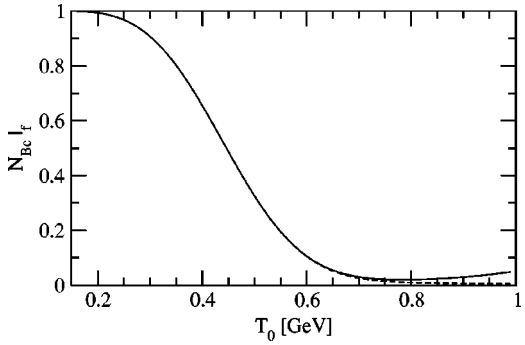

FIG. 6. Survival probability of an initial B_c as a function of initial temperature T_0 [GeV]; other parameters are the same as Fig. 3. Solid line: $N_c=10+$thermal production, dashed line: $N_c=10$.

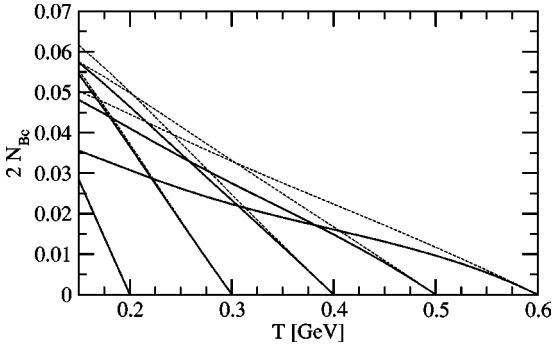

FIG. 7. B_c fractional abundance vs temperature [GeV] for various T_0 until freeze-out. Dashed line: $\rho_g=\frac{1}{2}\rho_g^{\infty}$. Other parameters are the same as Fig. 3.

initial temperature ($T\lesssim 350$ MeV) the state will most likely remain bound, while already at $T\gtrsim 500$ MeV the plasma will most likely dissolve the B_c. One can infer from this result that the final state population is mainly dominated by the formation process as the plasma cools between these temperatures. This of course is not in exact correspondence with the actual physical process, which involves the formation of the bound state at any time after QGP forms at the initial temperature, where the expansion has already produced a partial decrease in the gluon density.

Another way to interpret the results shown in Fig. 6 is that the effective collision-mediated color screening is most effective in dissolving B_c bound state when the average gluon energy $\overline{E}_g\simeq 3T$ exceeds the binding energy. Using this argument we can also easily see that the flavor transfer reaction $\overline{b}s+c\rightarrow\overline{b}c+s$ is unlikely, since the $\overline{b}s$ bound states have much smaller binding energies and are color screened already at all temperatures above the hadronization temperature.

B. Fractional B_c yields

We numerically integrate the evolution of the B_c abundance as function of the temperature T, using our expansion model to obtain the temperature as a function of time. The initial conditions are $N_{B_c}=0$ and $N_b=1$. We use $N_{c_0}=10$ and the volume expansion model for the charm quark density, and a full thermal gluon density. The final B_c population per initial $b\overline{b}$ pair is shown in Fig. 7. The factor of 2 in the axis label indicates that on average an equal number of particle and antiparticle bound states will be produced. Thus the numbers can be directly compared with the bound state ratio $10^{-4}-10^{-5}$ expected if no deconfinement occurs.

The nominal initial volume and expansion parameters are used. We explore a range $0.2\leqslant T_0\leqslant 0.6$ GeV of initial temperature in steps of 0.1 GeV. We see that the B_c abundance grows approximately linearly during the entire expansion as temperature decreases. This verifies that the formation and dissociation reactions do not come to equilibrium during the QGP phase, as previously anticipated in [4]. This linearity is not of any inherent physical origin, as can be seen by changing variables in Eq. (1) from τ to T and noting that $N_{B_c}\ll N_b$. The linearity in T is seen to follow from the numerical

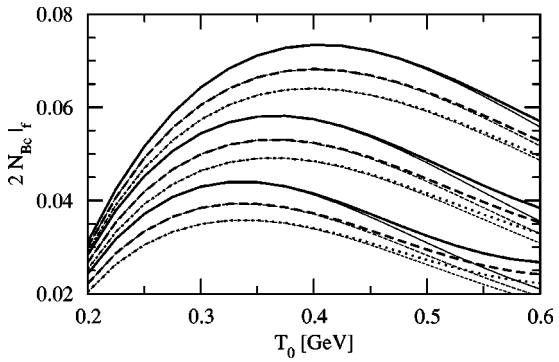

FIG. 8. B_c fractional abundance at freeze-out vs T_0 for $v_r = 0.58c$ (solid), $v_r = 0.79c$ (dashed), $v_r = c$ (dotted), and $V_0 = 26$ fm^3 (upper six lines), 52 fm^3 (middle six lines), 105 fm^3 (lower six lines). The effect of neglecting additional charm production in the QGP is shown in the thin lines which are only visible for $T \geqslant 0.5$ GeV.

values of the product $\dot{T}[\tau]\,V[\tau]\,\lambda_F$ remaining almost constant for $T_0 \lesssim 0.6$ GeV. The important conclusion we draw from the results shown in Fig. 7 is that we can expect a rather T_0 independent fractional B_c yield, which for the main benchmark of our assumptions is at 5%.

Shown by dashed lines in Fig. 7 is the scenario where gluon density is 1/2 its thermal equilibrium value $\rho_g^{\infty}(T)$. This corresponds to an effective reduction in the available degrees of freedom for gluons in a QGP for temperatures that are not yet ''asymptotically'' large [15]. One sees the expected effect of reduced gluon density leading to reduced dissociation, and hence increased final bound state populations. However, the increase is substantially less than linear, indicating that the formation term in the rate equation is dominant.

In order to better understand this result, and also to illustrate the dependence on initial QGP volume and transverse velocity, we show in Fig. 8 the freeze-out fractional B_c yield per one bottom quark pair, as a function of T_0, while also varying the other parameters.

As T_0 increases, the yield initially increases. However, as the initial temperature further increases, the dissociation reaction becomes more prominent and adversely impacts the yield, an effect which is not fully compensated by the additional QGP-produced charm available at these temperatures. This is seen comparing the thick up-curving lines with thin lines which do not include QGP-produced charm. However, this competition between formation and dissociation does lead to a very broad yield maximum in the vicinity of the expected range of initial temperatures at RHIC. This effect has been noted for the nominal expansion and initial volume parameters in Fig. 7. Here we see this effect persists for a variety of these parameters.

In order to establish a lower limit for the final B_c fractional abundance, we show by the dashed and dotted curves in Fig. 8 the effects of increasing the expansion rate, thus decreasing the lifetime of the QGP. We see that this effect is less than that generated by a change in initial volume, which controls the formation rate through the change in charm quark density. The different initial volumes are controlled by

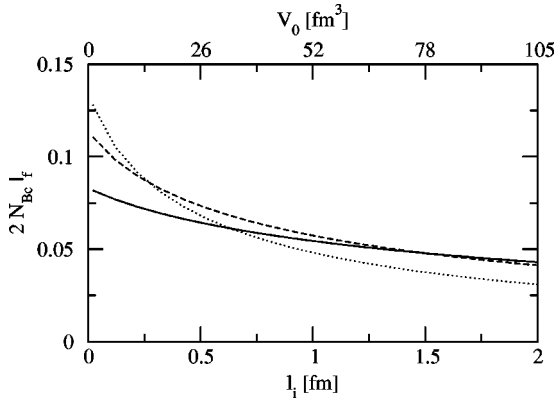

FIG. 9. B_c fractional yield at freeze-out as a function of the initial (width) parameter l_i [fm] for $T_0 = 0.5$ GeV (dotted), 0.4 GeV (dashed), and 0.3 GeV (solid).

varying l_i. The set of six lines in the middle corresponds to $l_i = 1$ fm ($V_0 = 52$ fm^3), our standard scenario, while the upper set of lines corresponds to the high density case $l_i = 0.5$ fm ($V_0 = 26$ fm^3) and the lower set of lines represents the low density case, $l_i = 2$ fm ($V_0 = 105$ fm^3).

In all of these calculations we have used an initial charm quark number $N_{c_0} = 10$, and for the range of temperatures expected at RHIC, this number will not change appreciably during the QGP lifetime. Eq. (1) then predicts that N_{B_c} will be exactly linear with the initial number of charm quarks, and our numerical results verify this. The calculated final B_c yields utilizing the average initial N_{c_0} thus will correctly include the fluctuations expected according to a binomial (or Poisson) distribution. This linear property is not evident in the results shown in Fig. 8 in terms of the initial charm density, since there one is changing the density by changing the volume, and this also effects the lifetime of the QGP and through that the final B_c abundance.

Shown in Fig. 9 is the fractional B_c-yield dependence on initial volume measured through variation of l_i for a range of initial temperatures. One sees that the temperature variation is less important than the initial volume effect, at least in the range of these parameters which we consider. For a fixed T_0, a change in the initial volume not only causes an inverse variation in the initial charm density $\rho_c \propto l_i^{-1}$, but also influences the plasma lifetime τ_L. Empirically it was found that $\tau_L \propto l_i^{1/2}$ is a good fit. These two factors combine to give the roughly $l_i^{-1/2}$ dependence of the final fractional B_c meson yield shown in Fig. 9.

C. Sensitivity to dissociation and formation cross sections

The dissociation cross section magnitude and shape is an essential part of our dynamical calculation, since in addition to providing a time scale, it provides through detailed balance the relative magnitude of the formation cross section. The form in Eq. (4) has been used to estimate the breakup rate of J/ψ due to final state collisions with hadrons, via convolution with the gluon structure function of the hadron [8]. Recently, there have been several additional attempts to model the hadron–quarkonium cross section [16], which has

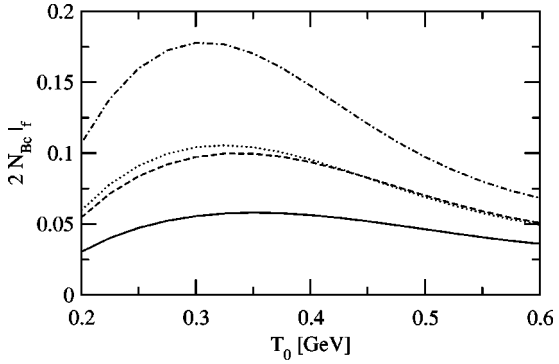

FIG. 10. B_c fractional yield at freeze-out for various theoretical breakup cross sections, nominal (solid), 2×nominal (dotted), constant (dashed), 2×constant (dotted-dashed).

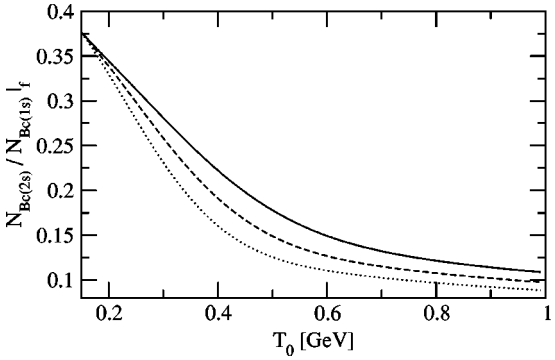

FIG. 11. Ratio of $B_c(2S)$ to $B_c(1S)$ abundance at freeze-out vs initial temperature [GeV] for $l_i=2$ fm (dotted line), 1 fm (dashed line), and 0.5 fm (solid line).

led to results which typically are much larger and have a more rapid rise above threshold. Here we investigate the sensitivity of our prediction B_c yields to such variations in the fundamental cross sections. We show in Fig. 10 the change in the predicted B_c yields at RHIC which follow if our breakup cross section in Eq. (4) is increased by a factor of 2. Also shown are corresponding results if the cross section is assumed to immediately rise to its maximum value just above threshold, with the same overall magnitudes as before. All other model parameters are kept at the nominal values. One sees that in all cases the final B_c yields are increased. One can understand this behavior as a combination of two effects. First, the detailed balance relation provides the relative magnitudes of formation and breakup rates. Second, an increase in the magnitude of the cross section just decreases the corresponding time scales, allowing the favored formation reaction to proceed further toward completion. Thus the cross section we have utilized provides a conservative lower bound for our B_c production estimates at RHIC via this new mechanism.

D. Relative excited state B_c yield

We have also calculated the ratio of $2S$ to $1S$-state B_c yields within our model scenario. This is prompted by the observation that the corresponding ratio in the charmonium system at SPS may serve as a thermometer of the QGP phase [17].

As a first estimate of this ratio we use as a $2S$ dissociation cross section (4) with $\epsilon_{2s}=0.25$ GeV. This of course is only a rough guess, since one should change the parameters to those corresponding to a $2S$ state, but this state has binding and energy levels which are very marginal in terms of the constraints used for the validity of the cross section formula. The individual population equations can be solved independently, since both final bound state fractions are small enough that the source of b quarks is not significantly decreased.

Figure 11 shows the ratio of yields $B_c(2S)/B_c(1S)$ at hadronization as a function of the initial temperature for the three different initial volumes we consider: $l_i=2$ fm (dotted line), 1 fm (dashed line), and 0.5 fm (solid line). It appears that this ratio is somewhat more sensitive to the initial temperature than the individual yields, varying by at least a factor of 2 within the expected range for RHIC.

We also find that this yield ratio is insensitive to initial charm abundance and production, as charm density enters linearly in both the $B_c(2S)$ and $B_c(1S)$ population equations. Also, the initial volume as shown in Fig. 11 does not alter the abundance ratio significantly. Thus this yield ratio may allow one to draw conclusions about initial temperatures present in the QGP phase at RHIC, independent of the other parameters. To estimate the systematic uncertainty that would arise in such a procedure, we consider the effects of changing the cross sections (formation and by detailed balance also breakup) in the following cases: (a) increasing the $(2S)$ cross sections by a factor of 2, (b) increasing both $2S$ and $1s$ cross sections by factor of 2, and (c) decreasing the $B_c(1S)$ and $B_c(2S)$ binding energies by 100 MeV. In all three cases the overall shape of the results as shown in Fig. 11 remain nearly unchanged. However, we note an overall increase in the relative yield by a factor of 2 in case (a), practically no change in the result in case (b), and a decrease by a factor of 1/3 in case (c). The ratio $B_c(2S)/B_c(1S)$ is thus primarily sensitive to initial temperature, but to be able to draw firm conclusions we need accurate relative $2S$ to $1S$ cross sections, and a good understanding of in-plasma B_c binding energy.

V. SUMMARY AND CONCLUSION

We have shown that this new mechanism of quarkonium production in a deconfined medium predicts the *minimum* final state abundance of B_c mesons at RHIC to be of the order of 5% per initial $b\bar{b}$ pair. This result is relatively insensitive to the initial temperature and volume of the QGP, as well as to changes in the transverse expansion dynamics. There is a linear dependence on the charm quark abundance in the initial state, which in fact is the primary controlling factor in the final state B_c yield.

Fractional B_c yields at the level of 5×10^{-2} significantly exceed expectations based on initial coherent one step production in individual nucleon–nucleon interactions, where a relative yield in the range of $10^{-4}-10^{-5}$ is expected. Such a small yield would not be observable at RHIC. Even the 500–1000 times greater multistep yield we obtain may pose con-

siderable experimental challenges. However, should such an experiment succeed to even roughly confirm these predictions for the fractional B_c yield, we would have a convincing evidence for the mobility of charmed quarks over an extended space–time region in the dense phase.

While in principle one could argue that incoherent B_c formation could also occur in the hadronic phase in collision of D mesons with B mesons, such a process requires localization in phase space of both these hadrons, which is highly unlikely. A calculation has been performed for the analogous case in the J/ψ system, using D-meson interactions [18]. It was found that this mechanism is negligible even at Large Hadron Collider (LHC) energies, except for possibly some observable effects in the ψ' yield.

We emphasize here that an essential element of this calculation relies on the assumption that colored heavy quarks will be subject to large energy loss processes in a plasma [19]. This is necessary if these heavy quarks are to exist in a common region of the phase space volume. Without this stopping, heavy quarks are highly unlikely to remain for the required period of time inside the thermal deconfined phase. The details of this scenario cannot be fully justified at present, and considerable effort has to be invested to better understand the mechanisms which determine the initial phase space distribution of heavy quarks formed in nuclear collisions.

Another issue is the final state reduction of B_c mesons due to collisions with comoving hadrons. However, we would expect the smaller size of these bound states relative to those extensively studied in the J/ψ system will produce a much less significant effect in the B_c system.

Our work relies heavily on the presence of mobile charmed quarks: investigation of other bound state formation, such as J/ψ, is currently underway. Initial results indicate that while a significant fraction of charm will be in fact bound (at the 10% level) this is too little to significantly alter the results we have presented for B_c yields. In fact the overall initial charm production uncertainty is at least as large as this effect. One such source is the possible shadowing of gluons in nuclei, which could reduce the primary yield by amounts in the tens of percents [20].

If the experimental techniques enable observation of these predicted B_c yields with significant efficiency, one has the possibility to embark upon a general study of both the vacuum and plasma properties of the B_c system. Even should this prove not to be possible in the RHIC energy range, it will most certainly be easier at the LHC, where the collision energy is 30 times greater. Several bottom quark pairs will be produced in each central nuclear collision, along with literally hundreds of charm quark pairs, leading to expectations involving copious production of B_c-mesons. A study of relevant parameters for this production mechanism at LHC is underway.

ACKNOWLEDGMENTS

This work was supported in part by a grant from the U.S. Department of Energy, Grant No. DE-FG03-95ER40937.

[1] CDF Collaboration, F. Abe *et al.*, Phys. Rev. Lett. **88**, 2432 (1998); Phys. Rev. D **59**, 032004 (1999).
[2] S.S. Gershteĭn, V.V. Kiselev, A.K. Likhoded, and A.V. Tkabladze, Phys. Usp. **38**, 1 (1995).
[3] For preliminary results on this subject see R.L. Thews *et al.*, hep-ph/9907424; S. Bass *et al.*, Nucl. Phys. **A661**, 248c (1999); L.P. Fulcher *et al.*, hep-ph/9905201.
[4] R.L. Thews, M. Schroedter, and J. Rafelski, Acta Phys. Pol. B **30**, 3637 (1999).
[5] K. Kolodziej and R. Ruckl, Nucl. Instrum. Methods Phys. Res. A **408**, 33 (1998). In this estimate the two lowest 1*S* (pseudoscalar and vector) states are included.
[6] P.L. McGaughey, E. Quack, P.V. Ruuskanen, R. Vogt, and X.-N. Wang, Int. J. Mod. Phys. A **10**, 2999 (1995).
[7] M.E. Peskin, Nucl. Phys. **B156**, 365 (1979); G. Bhanot and M. E. Peskin, *ibid.* **B156**, 391 (1979).
[8] D. Kharzeev and H. Satz, Phys. Lett. B **334**, 155 (1994).
[9] D. Kharzeev, nucl-th/9601029.
[10] Lewis P. Fulcher (private communication).
[11] See, for example, S.M.H. Wong, Phys. Rev. C **54**, 2588 (1996); **56**, 1075 (1997).
[12] J.D. Bjorken, Phys. Rev. D **27**, 140 (1983).
[13] J. Rafelski and J. Letessier, Phys. Lett. B **469**, 12 (1999).
[14] J. Letessier *et al.* (in preparation). For method, see J. Rafelski, J. Letessier, and A. Tounsi, Acta Phys. Pol. B **27**, 1035 (1996), and references therein.
[15] J.-P. Blaizot, E. Iancu, and A. Rebhan, Phys. Lett. B **470**, 181 (1999).
[16] See, for example, K. Martins, D. Blaschke, and E. Quack, Phys. Rev. C **51**, 2723 (1995); S.G. Matinyan and B. Müller, *ibid.* **58**, 2994 (1998); K.L. Haglin, *ibid.* **61**, 031902 (2000); C.Y. Wong, E.S. Swanson, and T. Barnes, hep-ph/99120431; nucl-th/0002034; Z.W. Lin and C.M. Ko, nucl-th/9912046.
[17] H. Sorge, E. Shuryak, and I. Zahed, Phys. Rev. Lett. **79**, 2775 (1997).
[18] P. Braun-Munzinger and K. Redlich, hep-ph/0001008.
[19] For a review, see R. Baier, D. Schiff, and B.G. Zakharov, hep-ph/0002198.
[20] K.J. Eskola, V.J. Kolhinen, and C.A. Salgado, Eur. Phys. J. C **9**, 61 (1999).